

A Search Algorithm for Optimal Resistance Measurement Points in Testing Power TSV with Manufacturing Variation Cancellation

Yudai Kawakami

Graduate School of Environmental Informatics
Teikyo Heisei University
Nakano-ku, Tokyo 164-8530
e-mail : 323Q11101@edu.thu.ac.jp

Koutaro Hachiya

Graduate School of Environmental Informatics
Teikyo Heisei University
Nakano-ku, Tokyo 164-8530
e-mail : k.hachiya@edu.thu.ac.jp

Abstract - Test methods have been proposed to detect open defects in power TSVs (Through Silicon Vias) in 3D-ICs by measuring the resistances between power supply pads placed directly beneath TSVs under test. When the manufacturing variation of the resistance is large, the diagnostic performance of testing a TSV must be improved by measuring two resistances, the detection resistance and the cancellation resistance, the latter of which is utilized to cancel the manufacturing variation component. Since the combinations of selecting these two resistance measurement points from the power supply pads directly under all TSVs are enormous, the previous research proposed the empirical rules to select the measurement points instead of searching for the optimum ones. This paper presents a search method for a local optimum solution by hill-climbing method, using measurement points determined by the empirical rules as the initial solution.

I. INTRODUCTION

Semiconductor devices are becoming 3D to avoid the limits of miniaturization and the cost increase that accompanies miniaturization [1][2]. At present, 3D has become common, especially in GPU memory and image sensors [3][4], and for the time being, stacked 3D-ICs that connect multiple stacked chips with TSV (Through-Silicon Via) will be the mainstream. TSVs deliver not only signals but also power (power TSVs) [4]. Open defects in power TSVs can cause power supply voltage drops, leading to timing errors in logic circuits, for example. Therefore, it is considered necessary to test power TSVs before shipment.

In general, there are two approaches to test methods: functional test and structural test. Based on the functional test approach, [5] proposes a method to measure the power supply voltage at various points in the power distribution network by voltage measurement circuits on a chip. Based on the structural test approach, [6] proposes placing power supply pads directly under power TSVs and measuring the resistance between these pads to detect open defects in power TSVs.

In the latter method, the resistance between power pads differs from device to device due to manufacturing variations. Since the resistance variation can cause false diagnosis, we find the measurement terminals (power pads) that maximize diagnostic performance. Initially, the most inefficient exhaustive search was adopted to optimize measurement terminals, but later, [7] proposed to use more efficient hill-climbing and neighborhood exhaustive search.

Even if the measurement terminals are optimized as described above, the probability of false diagnosis increases if the manufacturing variation in the resistance between power pads is large. Therefore, when testing one power TSV, a method has been proposed in which resistance measurements are performed twice, one to detect open defects and the other to cancel manufacturing variations [8]. However, these four terminals for the resistance measurements were selected by empirical rules found based on limited experimental results.

This paper proposes a method to optimize the four terminals to measure the two resistances when the manufacturing variation cancellation is applied. Section II summarizes contributions of the paper. Section III explains the test method for power TSVs and the manufacturing variation cancellation. The following section will explain how to select resistance measurement terminals based on the empirical rules. Section V describes the proposed method, and VI demonstrates the experimental results. Finally, section VII presents the conclusions.

II. CONTRIBUTIONS OF THIS WORK

This paper makes the following contributions regarding the search for resistance measurement terminals for power TSV testing methods when manufacturing variation cancellation is performed, as shown in III.

- This paper proposes a local optimization method using the hill-climbing method to find the measurement terminals, while only empirical rules have been proposed for the purpose so far.
- Comparing the diagnostic performance of the solution (i.e. measurement terminals) obtained using the empirical rule and the true optimal solution, it is shown that relatively high performance can be obtained even with the empirical rule.
- Comparing the solution obtained by the proposed method and the solution obtained by the empirical rule, it is shown that there are cases where the empirical rule solution is improved.
- Comparing the diagnostic performance of the solution obtained by the proposed method and the true optimal solution, it is shown that the proposed method can achieve sufficiently high performance.

III. TEST METHOD FOR POWER TSVs

Fig. 1 shows a schematic cross-section of the power distribution network of a 3D-IC [8]. Power TSVs connect two VDD distribution networks in different dies (KGDs, Known Good Dies). Furthermore, power pads are arranged directly under these TSVs. When an open defect occurs in TSV 1_7 in the center of Fig. 1, the resistance between power supply pads 1_7 and 1_13 changes from the value when there is no open defect. On the other hand, the resistance between power supply pads 1_8 and 1_13 hardly changes, even if an open defect occurs in TSV 1_7.

Using the resistance change between the power supply pads as described above, the TSV open defect is tested in the following procedure [6].

- 1) Place a power supply pad directly under each power TSV.
- 2) Find resistance measurement terminals (power supply pad pair) so that the measured resistance R_d can detect the open defect of each power TSV with sufficient diagnostic performance.
- 3) Determining the resistance threshold for each power TSV considering the defect coverage and yield loss.
- 4) Measure the resistances between corresponding pairs of power supply pads to detect open defects in all power TSVs. Diagnose as a defect when the resistance value exceeds the threshold.

As the diagnostic performance used in 2), this paper uses RMD (relative mean difference) defined by the following equation:

$$RMD = \frac{\mu_2 - \mu_1}{\sigma_1 + \sigma_2}$$

where μ_1 and σ_1 are the mean and standard deviation of R_d when there is no open defect in TSV under test, and μ_2 and σ_2 are the mean and standard deviation of R_d when an open defect occurs in the TSV. If the RMD value is small, the probability of false diagnosis increases. Ref. [7] proposed *hill-climbing* and *exhaustive neighborhood search* as methods for searching for the optimal measurement terminals in 2) above. If we cannot find a pair of resistance measurement terminals with sufficient diagnostic performance even after the optimization, the following manufacturing variation cancellation method is applied.

In addition to the *detection resistance* R_d in 2) above, find the measurement terminals of the *cancellation resistance* R_c with the following two characteristics [8].

- Strong correlation between manufacturing variation of R_d and R_c
- When an open defect occurs in the TSV under test, the change in the R_c is negligible compared to the change in the R_d .

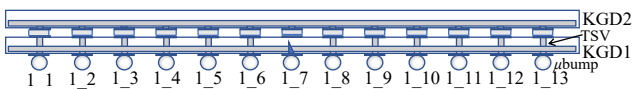


Fig. 1. Cross section of power distribution network in 3D-IC [8].

Then, instead of R_d , $R_{diff} = R_d - a \cdot R_c$ is used to detect the open defect where a is determined by linear regression analysis $R_d \approx a \cdot R_c + b$, which approximates R_d when there are no open defects.

IV. EMPIRICAL RULES FOR SELECTING MEASUREMENT POINTS (CONVENTIONAL METHOD)

In the previous research, we selected the measurement terminals of the detection resistance R_d and the cancellation resistance R_c using the following empirical rules without searching for the optimum measurement terminals [8]. In the following, $R(i, j)$ represents the resistance between power supply pads i and j .

Select the detection resistance $R_d = R(d_1, d_2)$ and the cancellation resistance $R_c = R(c_1, c_2)$ according to the following rules.

- For d_1 , choose the power pad closest to the TSV under test.
- For d_2 , choose the power pad farthest from d_1 .
- For c_1 , choose the second closest power pad to the TSV under test.
- For c_2 , select the same pad as for d_2 .

The above rules were empirically obtained by manually optimizing the measurement terminals for some TSVs in the experiment [8]. The validity of the above rules can be explained qualitatively as follows. In selecting d_1 and d_2 , the rules choose the resistance measurement terminals so that the current flowing through the TSV under test becomes maximum during R_d measurement. This makes the resistance change as large as possible when an open defect occurs. The rules select c_1 and c_2 so that the measurement terminals are as close as possible to d_1 and d_2 . As a result, the rules maximize the correlation between manufacturing variations of R_d and R_c .

V. PROPOSED HILL-CLIMBING METHOD

We propose to apply the *hill-climbing* method even when the manufacturing variation cancellation method is applied, following the measurement terminal optimization method when the manufacturing variation cancellation method is not applied. As the initial solution of the hill-climbing, we use the measurement terminals selected by the empirical rules explained in IV. In the following, we will explain the proposed optimization method using the pseudo-code in Fig. 2.

At the second line of the pseudo-code, four measurement terminals (d_1, d_2, c_1, c_2) are determined using the conventional empirical rules for the TSV under test (T_{SVUT}) given by the argument. Substitute the list of the four terminals into $bestPads$ as the initial solution for the hill-climbing method.

The procedure $Eval$, which is called in the 3rd and 8th lines, obtains the R_{diff} after canceling the manufacturing variation and calculates the diagnostic performance RMD . To calculate RMD , it is necessary to run a Monte Carlo circuit simulation three times to get R_d and R_c when there is no defect and R_d

```

1: function HillClimbing(TsvUT)
2:   bestPads = EmpiricalRules
3:   bestRMD = Eval(bestPads)
4:   while(true)
5:     nextPads = NULL
6:     nextRMD =
7:     for each (x in Neighbors(bestPads))
8:       if (nextRMD < (RMD=Eval(x)))
9:         nextRMD = RMD
10:        nextPads = x
11:   if (nextRMD <= bestRMD)
12:     return bestPads
13:   bestPads = nextPads
14:   bestRMD = nextRMD

```

Fig. 2. Pseudo-code of hill-climbing

when there is an open defect in TsvUT.

The procedure `Neighbors` in the 7th line derives the sets of adjacent power pads to each d_2 , c_1 , and c_2 out of the four terminals in $\text{bestPads} = (d_1, d_2, c_1, c_2)$. Then it enumerates all combinations of elements of these sets and puts them into a list (excluding bestPads). That is, it generates a list of the elements in the set below:

$$\{ (d_1, k, l, m) \mid \forall k \in \text{adj}(d_2), \forall l \in \text{adj}(c_1), \forall m \in \text{adj}(c_2) \} \setminus \{ (d_1, d_2, c_1, c_2) \},$$

where $\text{adj}(p)$ represents the set that includes the power pad p and all power pads physically adjacent to p . However, if the set $\text{adj}(p)$ includes d_1 , it is deleted from $\text{adj}(p)$, and all the power pads adjacent to d_1 are added to $\text{adj}(p)$ instead. Replacing d_1 with its neighbors in $\text{adj}(p)$ prevents k , l , and m from becoming d_1 and allows them to move beyond d_1 . The operator “\” represents the set difference.

VI. EXPERIMENTAL RESULTS

Using the same 3D-IC structure shown in Fig. 1 and experimental conditions used in the experiment in [7] and [8], we obtained the resistance measurement points to test all 70 TSVs with manufacturing variation cancellation by *exhaustive search*, the *empirical rules* and the proposed *hill-climbing*. We compare how these methods affect diagnostic performance *RMD* and runtime of the search methods.

A. Simulation Setup

We assume that there are two power distribution networks within a chip, VDD and GND, but only VDD is considered here. Both dies in the 3D-IC are 13 mm square, and the power distribution networks of the two dies have the same structure shown in Fig. 3. The M7 layer (vertical) and M6 layer (horizontal) metal constitute a power grid network. The resistor model in Table I is used for the resistance of the wire segments that make up the power grid. We assume that the variation of wire width W and wire thickness T caused the manufacturing variation in the resistance. In the experiment, all wire segments in the same layer have the same W and T , and W and T in different layers vary independently according

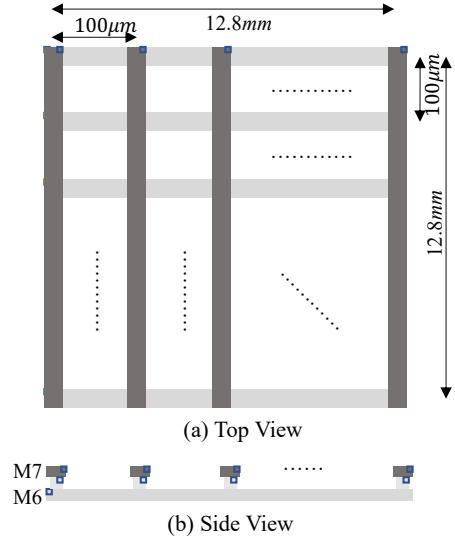


Fig. 3. Power grid dimensions [8].

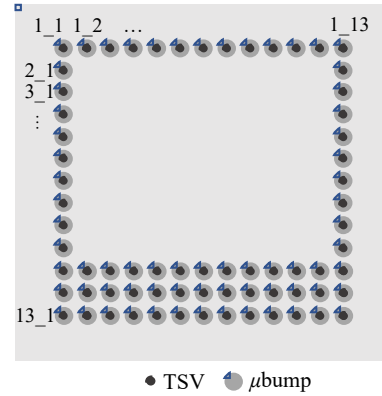


Fig. 4. Positions of power TSVs and power pads [6].

to a normal distribution. Also, the via resistance connecting M7 and M6 is ignored in this experiment.

We placed 70 TSVs and 70 pads, as shown in Fig. 4. Marks 1_1 and 13_13, for example, in Fig. 4 express their positions in the format “(row number)_(column number).” All of them are directly under the intersection of the power grid in the dies. TSVs are cylindrical, and R_{TSV} in Table I models their resistance. The radius r is assumed to vary independently for each TSV with a normal distribution. We handle only open defects among TSV defects, and the resistance is set to $R_{\text{open}}=10^{12} (\Omega)$ when the open defect occurs in a TSV.

We performed DC operating point analysis using a circuit simulator when deriving the detection resistance R_d and the cancellation resistance R_c . We used SPICE3 [9] enhanced with an accelerated linear equation solver and a Monte Carlo analysis function. We performed Monte Carlo analyses to obtain the average and standard deviation of the resistances. The number of Monte Carlo trials was 3,000, and the Latin Hypercube was used as the sampling method. The netlist for performing these circuit simulations was created manually,

TABLE I. RESISTANCE MODEL USED IN THE EXPERIMENT

Resistance model			
Symbol	meaning	Model equation	
R_{wire}	resistance of a wire segment	$\rho l/(WT)$	
R_{TSV}	resistance of a TSV	$\rho l/(\pi r^2)$	
Constants			
Symbol	meaning	value	
ρ	conductivity of Cu	$1.68 \times 10^{-8} (\Omega\text{m})$	
l	length of wire seg. and TSV	100 (μm)	
Variable parameters			
Symbol	meaning	mean	coef. of variation
W	wire width	3 (μm)	5%
T	wire thickness	3 (μm)	5%
r	TSV radius	1 (μm)	5%

containing 65,606 resistance elements and 33,281 nodes.

We implemented the proposed hill-climbing in Python. In addition to the proposed method, we implemented another optimization program by exhaustive search in Python for comparison. These measurement point optimization programs and the circuit simulator are run on Apple iMac (Intel Core i9 3.6GHz, 64GB 2667MHz DDR4).

B. Improvement in Diagnostic Performance

Table II shows the resistance measurement terminals (power pads) obtained by the proposed method and the RMD value when tested with those terminals. The table only shows 18 TSVs out of 70 due to space limitations. For comparison, the table also shows the "true optimum" obtained by the exhaustive search method and the resistance measurement terminals obtained by the "empirical" rule of the conventional method. Of the 70 TSVs, the proposed method improved the RMD from the conventional method in 36, which is about half. RMD increased by up to 0.199 (the max. occurs at TSV 1_2). There were 60 cases where the resistance measurement terminals obtained by the proposed method were different from the true optimum. As a result, the RMD is slightly lower than the true optimum, but the maximum is only 0.069, which is a 1.03% relative error (at TSV 1_5).

C. Runtime

Table III shows the execution time when searching for resistance measurement terminals for all 70 TSVs using the proposed method. Since the conventional empirical method does not need to search for the optimum, its processing time is negligible. Instead of the empirical method, the execution time by the exhaustive search is shown in that table. The run time for the exhaustive search was obtained by multiplying the time required to derive RMD from the simulation results, 0.145 seconds, by the number of all combinations of the four measurement terminals. Note that the runtime in Table III does not include the circuit simulation runtime. The number of circuit simulation runs (#Sim.) was 9,660 (4,830 without defects, 4,830 with faults) for the exhaustive method and 564 (332 without defects, 232 with defects) for the proposed method. The average execution time for one circuit simulation

TABLE III. RUNTIME OF THE PROPOSED METHOD.

	Exhaustive search	Hill-climbing	speedup
runtime	1,647,780 sec	564 sec	2,921
#Sim.	9,660	564	17.1

was 1,061 seconds.

VII. CONCLUSIONS

The resistance measurement terminals obtained by the proposed method showed an improvement in RMD for about half the TSV compared to the conventional method based on the empirical rules. In addition, the results of the proposed method did not show a significant difference in RMD compared to the true optimum (approximately 1% or less relative error).

However, running the circuit simulation while searching for the solution is necessary for the proposed method, and the cost is much higher than the empirical rules. Therefore, it is better to search for the measurement terminals by the proposed method only when the RMD requirements cannot be met with the measurement terminals determined by the empirical rules.

ACKNOWLEDGEMENTS

This work was supported by JSPS KAKENHI Grant Number JP19K11883.

REFERENCES

- [1] K. N. Tu, "Reliability challenges in 3D IC packaging technology," *Microelectronics Reliability*, 51(3), pp. 517-523, 2011.
- [2] M. Aoyagi et al., "Developing a leading practical application for 3D IC chip stacking technology," *Synthesiology English edition*, 9(1), pp. 1-15, 2016.
- [3] Lu, M. "Advancement of chip stacking architectures and interconnect technologies for image sensors," *ASME. J. Electron. Packag.*, 144(2), June 2022.
- [4] H. Park et al., "Transformer network-based reinforcement learning method for power distribution network (PDN) optimization of high bandwidth memory (HBM)," *IEEE Trans. on MTT*, 70(11), pp. 4772-4786, Nov. 2022.
- [5] S. Huang, "Test strategies for the clock and power distribution networks in a multi-die IC," *International Symposium on VLSI-DAT*, pp. 1-2, April 2017.
- [6] K. Hachiya and A. Kurokawa, "Open Defect Detection of Through Silicon Vias for Structural Power Integrity Test of 3D-ICs," *IEEE 23rd Workshop on Signal and Power Integrity*, pp. 1-4, June 2019.
- [7] K. Hachiya, "Measurement Point Selection Algorithms for Testing Power TSVs," *2023 IEEE International 3D Systems Integration Conference (3DIC)*, pp. 1-4, May 2023.
- [8] K. Hachiya and A. Kurokawa, "Testing Through Silicon Vias in Power Distribution Network of 3D-IC with Manufacturing Variability Cancellation," *Design, Automation & Test in Europe Conference & Exhibition (DATE)*, pp. 290-293, March 2020.
- [9] Rabaey, J. M.: *The Spice Page*, EECS Department of the University of California at Berkeley (online), available from <http://bwrcs.eecs.berkeley.edu/Classes/IcBook/SPICE/> (accessed 5th August, 2023).

TABLE II. MEASUREMENT POINTS AND DIAGNOSTIC PERFORMANCE RMD DERIVED BY THE PROPOSED METHOD.

TSV, d_1	True optimum			Empirical (conventional)			Hill-climbing (proposed)				
	$d_2(=c_2)$	c_1	RMD [†]	$d_2(=c_2)$	c_1	RMD [*]	$d_2(=c_2)$	c_1	RMD	RMD-RMD [*]	RMD-RMD [†]
1_1	7_13	12_3	7.075	13_13	2_1	7.030	13_13	2_1	7.030	0.000	-0.046
1_2	13_2	1_3	6.803	13_13	1_1	6.580	13_13	1_3	6.780	0.199	-0.023
1_3	13_13	1_2	6.771	13_13	1_2	6.771	13_13	1_2	6.771	0.000	0.000
1_4	13_5	1_3	6.732	13_13	1_3	6.718	13_13	1_3	6.718	0.000	-0.013
1_5	7_1	12_6	6.696	13_13	1_4	6.623	13_13	1_6	6.627	0.004	-0.069
1_6	7_1	11_6	6.705	13_13	1_5	6.678	13_13	1_5	6.678	0.000	-0.027
1_7	7_13	12_6	6.658	13_1	1_6	6.578	13_2	1_8	6.646	0.067	-0.013
2_1	7_13	12_2	6.789	13_13	1_1	6.629	13_12	3_1	6.734	0.105	-0.054
2_13	8_1	12_10	6.768	13_1	1_13	6.680	13_2	3_13	6.718	0.038	-0.050
3_1	7_13	12_2	6.760	13_13	2_1	6.721	13_1	2_1	6.721	0.000	-0.039
3_13	7_1	12_12	6.757	13_1	2_13	6.689	13_1	2_13	6.689	0.000	-0.068
12_7	1_5	12_8	6.354	1_1	11_7	6.228	1_1	12_8	6.348	0.121	-0.006
12_8	1_2	12_9	6.404	1_1	11_8	6.233	1_2	12_9	6.404	0.171	0.000
12_9	1_6	12_10	6.375	1_1	11_9	6.223	1_1	12_10	6.362	0.138	-0.014
12_10	2_13	12_9	6.424	1_1	11_10	6.344	1_1	12_9	6.382	0.037	-0.043
12_11	1_1	12_12	6.366	1_1	11_11	6.296	1_1	12_12	6.366	0.069	0.000
12_12	1_13	12_11	6.424	1_1	11_12	6.347	1_2	12_11	6.392	0.046	-0.031
12_13	12_1	12_12	6.654	1_1	11_13	6.549	1_1	12_12	6.629	0.080	-0.025